Research Article Vol. 10, No. 7 | 1 Jul 2019 | BIOMEDICAL OPTICS EXPRESS 3463

Biomedical Optics EXPRESS

Monitoring of individual bacteria using electro-photonic traps

DONATO CONTEDUCA,[1,2] **GIUSEPPE BRUNETTI,**[1] **FRANCESCO DELL'OLIO,**[1] **MARIO N. ARMENISE,**[1] **THOMAS F. KRAUSS,**[2] **AND CATERINA CIMINELLI**[1]

[1]*Optoelectronics Laboratory, Politecnico di Bari, Via Orabona, 4, 70125, Bari, Italy*
[2]*Photonics Group, Department of Physics, University of York, Heslington, York, YO10 5DD, UK*
**caterina.ciminelli@poliba.it*

Abstract: Antimicrobial resistance (AMR) describes the ability of bacteria to become immune to antimicrobial treatments. Current testing for AMR is based on culturing methods that are very slow because they assess the average response of billions of bacteria. In principle, if tests were available that could assess the response of *individual* bacteria, they could be much faster. Here, we propose an electro-photonic approach for the analysis and the monitoring of susceptibility at the single-bacterium level. Our method employs optical tweezers based on photonic crystal cavities for the trapping of individual bacteria. While the bacteria are trapped, antibiotics can be added to the medium and the corresponding changes in the optical properties and motility of the bacteria be monitored via changes of the resonance wavelength and transmission. Furthermore, the proposed assay is able to monitor the impedance of the medium surrounding the bacterium, which allows us to record changes in metabolic rate in response to the antibiotic challenge. For example, our simulations predict a variation in measurable electrical current of up to 40% between dead and live bacteria. The proposed platform is the first, to our knowledge, that allows the parallel study of both the optical and the electrical response of individual bacteria to antibiotic challenge. Our platform opens up new lines of enquiry for monitoring the response of bacteria and it could lead the way towards the dissemination of a new generation of antibiogram study, which is relevant for the development of a point-of-care AMR diagnostics.

© 2019 Optical Society of America under the terms of the OSA Open Access Publishing Agreement

1. Introduction

The major cause for the increase of bacterial infections is their ability to resist antimicrobial treatments [1], termed antimicrobial resistance (AMR). The threat of AMR has increased significantly in recent years due to the overuse and incorrect prescription of antibiotics. The cost of AMR on Public Health is estimated at around 1.5 billion Euro in the European Union alone and AMR is expected to become the leading cause of death worldwide with over 10 million annually predicted by 2050 [2] unless new solutions can be found. A key such solution is the development of a better diagnostic test, i.e. a test that enables the determination of the correct antibiotic to be used on a short timescale, i.e. ideally below 30 mins, so there is a clear need to find novel diagnostic techniques that can rapidly identify the most suitable antibiotic for a given infection.

To date, the most widely used diagnostics is the plate-count method, based on the growth of bacteria on an agar plate in the presence of different antibiotics [3]. This technique is time-consuming (24-72 hours) because it requires many cell-division cycles; expert users are also required for sample preparation and final analysis [4]. The time-delay is the critical issue, however, because some infections such as sepsis require immediate attention [5] and, more generally, clinicians administer antibiotics based on experience rather than accurate diagnosis, which has a significant error rate.

As a result, a significant research effort is being directed towards finding new methods for detecting the response of individual bacteria in real-time. For example, techniques such as

#362499 https://doi.org/10.1364/BOE.10.003463
Journal © 2019 Received 15 Mar 2019; revised 17 May 2019; accepted 20 May 2019; published 19 Jun 2019

Surface Enhanced Raman Spectroscopy (SERS) and fluorescence techniques have been demonstrated with good success. However, these methods are not label-free, so they require the species-specific functionalization of bacteria, which is difficult, especially as bacteria readily mutate. Because of their fast mutation rate, bacteria of apparently identical makeup may respond differently to antibiotics, such that both resistant and susceptible bacteria may bind to the same fluorescent molecule [6].

Instead of using functionalisation to identify or localise bacteria, we now propose to use optical cavities to trap them. The strong trapping force available with such cavities [7] provides high sensitivity to any changes in the bacterial properties. For example, plasmonic cavities [8] and photonic crystal (PhC) cavities [9,10] have been demonstrated to trap, detect and characterize single-cell bacteria with a very fast and label-free approach [9].

Because of the large variety of pathogenic bacteria and the correspondingly large number of different antibiotics needed to challenge them, and their different modes of operation (some antibiotics stop growth, while others lyse the cell etc.), a single interrogation technique is not sufficient for a full assessment of antibiotic susceptibility. As a result, multiple methods should be used in parallel, leading to a multiparameter approach. In particular, electrical methods are promising [11]; as a case in point, it has been known for a long time that the impedance of the cell culture medium changes as a function of bacterial metabolic activity [12,13].

Several configurations of electrical biosensors have been realized to detect and characterize bacteria via their metabolic activity. For example, impedance flow cytometry [14] is used to distinguish between dead and live bacteria without requiring any labelling as for fluorescence-based approaches. Amongst other electrical methods, Electrochemical Impedance Spectroscopy (EIS) with configurations based on interdigitated microelectrodes has demonstrated the lowest detection limit down to 10 CFU/mL [15,16] and a clear change in impedance has been observed when exposing bacteria to antibiotics [17]. Although these examples indicate the suitability of electrical techniques for the study of bacterial infections, they typically operate at the bacterial community level and require cell growth with concentrations in the 10^5-10^6 CFU/mL range [18] to obtain a detectable change of impedance.

Here, we propose a new electro-photonic system that combines integrated optical tweezers with electrical impedance measurements, which enables a much faster antibiogram study preserving the information from each individual microrganism by monitoring the metabolic state in order to assess antibiotic susceptibility to different antitbiotics [19].

The system consists of an array of optical tweezers to trap many bacteria in parallel, thereby combining the assessment of optical density with the assessment of bacterial motility and electrical impedance measurements in a multiparameter format. Our simulations show that even for a moderate Q-factor of $Q \approx 2000$, strong and stable trapping is achieved. Additionally, and by realizing the cavities in doped silicon with interdigitated contacts, we predict a variation in measurable electrical current by up to 40% between live and dead bacteria, thereby facilitating the assessment of bacterial metabolism via impedance measurements.

2. Design of the electro-photonic trap

2.1. Photonic design

The electro-photonic trap is realized as a photonic crystal cavity of the well-known “L3”-type (Fig. 1 and Fig. 2) realized in silicon-on-insulator (SOI) technology. The cavity is far-field optimised to allow out-of-plane excitation [20] which affords the excitation in the normal direction and is easily scalable into an array-format. The detailed design of the cavity is described in the Appendix.

Trapping a single bacterium increases the effective index in the cavity mode thereby red-shifting the cavity resonance (see Fig. 2 and Fig. 3) [21]. The magnitude of the resonance shift can also be used to identify whether the bacterium is Gram positive or Gram negative, because of their different size and optical density [14,21]. The strong optical gradient available with the photonic crystal cavity approach maximises the trapping force and minimises the optical power required to achieve trapping, thereby minimising phototoxicity effects [22,23]. Since live and dead bacteria exhibit different optical properties, these changes also reflect the action of antibiotics [24]. For example, disruption of the cell wall occurs when antibiotics stop the bacteria growth with an inhibition of DNA, RNA and protein synthesis and their consequent release from the cytoplasm [25].

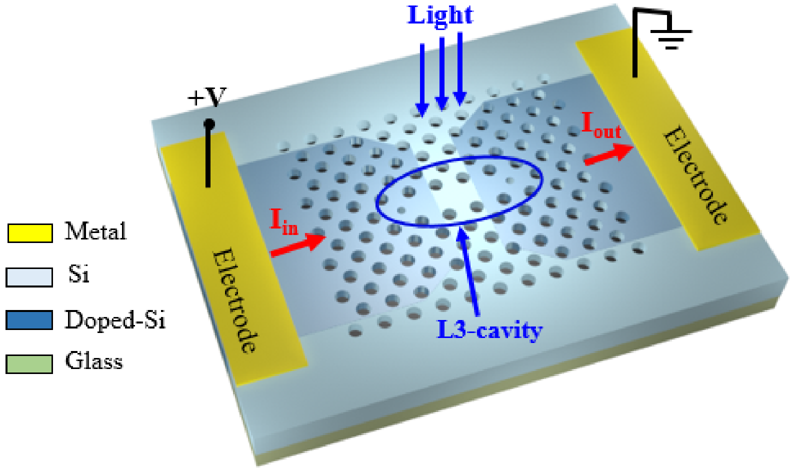

Fig. 1. (a) Schematic of the electro-optic trap based on a PhC L3-cavity as optical trapping site. The dark blue areas represent doped silicon and the light blue areas undoped silicon.

In addition to the wavelength shift, the time-dependence of the optical signal provides useful information on the motility of the bacterium. If the bacterium is trapped, it will primarily align with the cavity axis in order to occupy the energetically favourable high field regions. However, its motility will cause the bacterium to oscillate and rotate within the trapping potential, hence impart noise on the optical signal. Since antibiotic action impacts on motility, any changes in this time-dependent noise signature can be interpreted as a signature of antibiotic susceptibility.

Another benefit of optical trapping is that the tweezers locate the bacterium for extended periods of time, which allows us to monitor their electrical response to antibiotic challenge, as we will discuss next.

A Q-factor of few thousand ($Q < 10^4$) is chosen as the best compromise between optical forces and the probability of successfully trapping the bacteria [26]; higher Q-factors would allow stronger trapping action, but also a higher probability that the cavity is out-of-resonance due to the strong motility of bacteria. In fact, the movement of the bacterium in the trap changes the resonance condition with a consequent worsening of trapping force, so allowing them to escape. Conversely, lower Q-factors correspond to weak trapping efficiency, so reducing the trapping time [26].

The main advantage of using L3 cavities for optical trapping is that the area of the trapping site is comparable to the volume of a single bacterium (see Fig. 2). In this condition, assuming the electro-photonic traps integrated in a microfluidic channel with a continuous flow inside, only the microorganisms flowing close to the region with a strong evanescent field are trapped in the cavity. After the trap is full, there is not energy confined around the trapped bacterium, so preventing, or at least remarkably reducing the probability, that another bacterium will be trapped in the same region. By introducing several PhC L3 cavities in the sample and with a top-illumination approach, many trapping site will be activated at the same time, so enabling the simultaneous analysis of several bacteria locally trapped in well-defined positions of the chip.

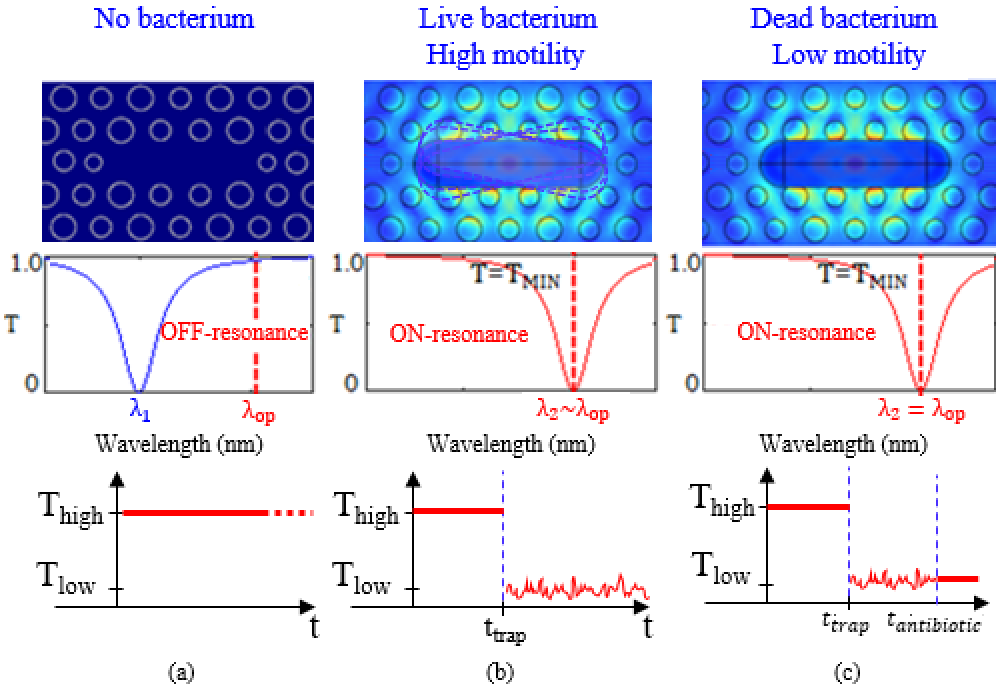
No bacterium
Live bacterium High motility
Dead bacterium Low motility
1.0
T
0
OFF-resonance
ON-resonance
T=T_MIN
λ1
λop
λ2~λop
λ2 = λop
Wavelength (nm)
T_high
T_low
t
t_trap
t_antibiotic
(a)
(b)
(c)

Fig. 2. Operating principle of the photonic system for the detection of individual bacteria. (a) The cavity is off-resonance when the bacterium is not trapped with an optical transmission T = T_{MAX}. (b) Following trapping, the cavity is on-resonance with optical transmission T = T_{MIN}, but with relevant noise due to the high motility of the bacterium. (c) When the trapped bacterium dies, the cavity resonance is still close to λ_{op} (T ~T_{MIN}) and the noise becomes weaker as the motility decreases.

Using a 3D Finite Element Method (FEM) model, we determine a cavity Q-factor of $2.3\text{x}10^3$ with a transmission dip of 29% on resonance, assuming the water absorption. Furthermore, we have studied the cavity behaviour as an optical tweezer. We represent the *E.coli* bacterium as a 2 µm long cylinder with a diameter of 500 nm and refractive index of $n_{bac} = 1.388$ [27]. The maximum force exerted onto the bacterium is 15pN close to the surface and the force drops off exponentially over 200 nm as expected from the exponential tail of the guided cavity mode.

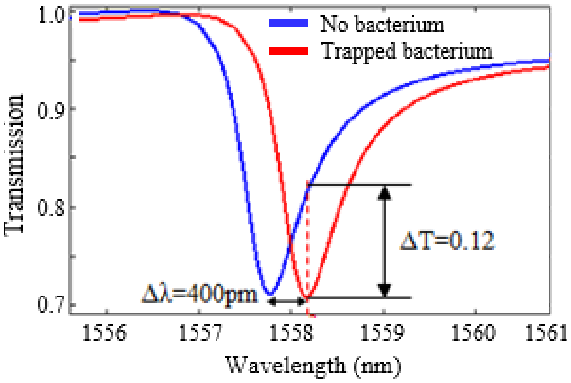

Fig. 3. Resonance shift after a single bacterium trapping event in the L3-cavity.

It is also interesting to consider the trapping force exerted by a nanophotonic cavity on the bacterium and compare it to the classical geometry of a Gaussian beam trap. To this end, we consider the optical stability defined as $S = \int_{r_0}^{\infty} F \cdot dr / \left(k_B T_c\right)$ where k_B is the Boltzmann constant, T_c is the temperature and the integral $\int_{r_0}^{\infty} F \cdot dr$ corresponds to the work necessary to bring the particle from a free position to the equilibrium point. A stability of S >10 is typically considered as resulting in a stable trap [28], so the power required to reach this stability is a good figure of merit for a trapping system.

Using the method described in [28], we calculate that the power density required to achieve S = 10 is 9.6×10^6 W/m^2. This value compares favourably to a Gaussian beam trap at the typical trapping wavelength of 1064nm (> 10^8 W/m^2 for S = 10) [29], which is over an order of magnitude higher. This comparison highlights that optical nanotweezers achieve significantly higher stability and/or lower power operation (resulting in lower phototoxicity) than conventional Gaussian beam traps.

2.2 Electrical design

The bacterium is probed by an AC field, which allows us to pick up changes in the impedance when it is challenged by an antibiotic. The equivalent electrical circuit is shown in Fig. 4. The model assumes that the membranes of the trapped bacterium are perforated by the antibiotic, so causing the ions release. Nevertheless, once the ions have been released, the impedance of the bacterium increases, which is detectable with a judicious choice of operating frequency. Typically, if f > 10 KHz, the membranes become electrically transparent and the bacterium can be modelled with a resistive behavior. Therefore, in the equivalent circuit of the device in Fig. 4, the electrical equivalent circuit of the vertical cross-section of the trapping region of can be described by a parallel configuration of three components: the silicon slab resistance $R'_{slab,}$ the resistance of the bacterium R_{bac} and the resistance of the surrounding medium (R_{sol}). Outside the trapping region, the silicon slab is heavily doped in order to confine the current flow to R_{slab}, so R_{sol} and R_{bac} do not need to be considered there. In the centre of the cavity, the silicon is undoped, represented by R'_{slab}, and the current is forced to flow through the medium in the region where the bacterium will be trapped.

The trapping event of a bacterium then causes a change of the electrical current passing through the system. More importantly, any changes in the electrical properties of the bacterium will directly impact on the measured electrical current, hence the current allows us to monitor the metabolic activity of the bacterium and therefore its susceptibility to antibiotic challenge.

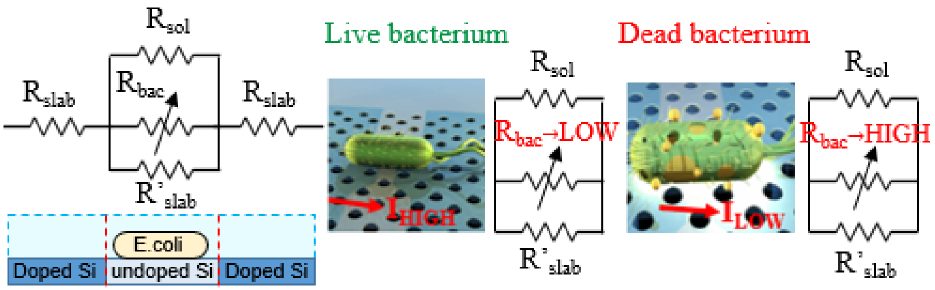
R_sol
R_slab
R_bac
R_slab
R'_slab
E.coli
Doped Si
undoped Si
Doped Si
Live bacterium
R_sol
R_bac→LOW
I_HIGH
R'_slab
Dead bacterium
R_sol
R_bac→HIGH
I_LOW
R'_slab

(a) (b) (c)

Fig. 4. Equivalent electrical circuit of (a) the cross-section of the electro-photonic device with (b-c) a focus in the region of trapping site, with R'_{slab} the resistance of the PhC silicon slab, R_{sol} the resistance of the surrounding solution, R_{bac} the resistance associated to the bacterium (b) R_{bac} is low when the bacterium is live and (c) high when the external membrane is disrupted by the antibiotics, which corresponds to high and low values of current, respectively.

We use a three-shell ellipsoidal model representing the cytoplasm, the inner membrane, the periplasm and the outer membrane (Fig. 5(a)) [30]. This model can be understood as a general representation of a gram-negative bacterium. The various parameters used to simulate a live and dead bacterium are described in [31], obtained experimentally by electrorotation. The model is based on the observation that the antibiotic provokes the perforation of the outer and also inner wall of the bacterium with a consequent release of ions and organelles from the cytoplasm and the periplasm [32]. Electrically, this means that a dead bacterium after the damaging of the membranes and without an intact periplasm and cytoplasm can be presented by an ellipsoid with the lower average conductivity of σ_{dead} = 9x10^{-2} S/m (see Fig. 5(b)), as verified experimentally in [31].

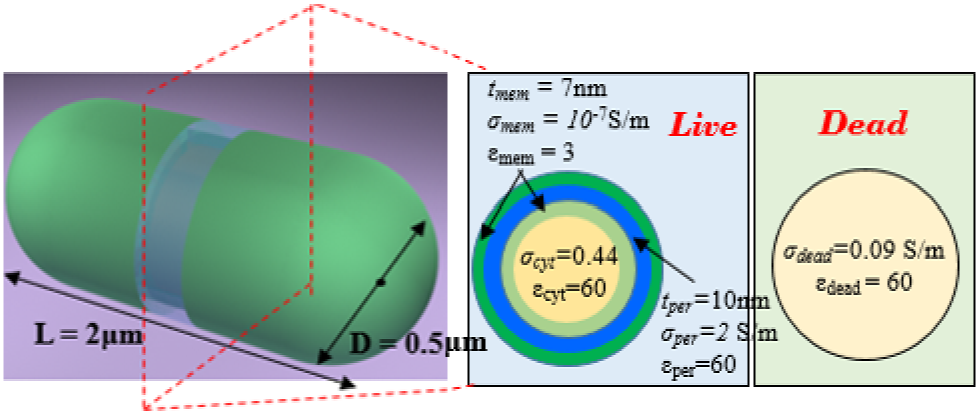
L = 2µm
D = 0.5µm
t_{mem} = 7nm
σ_{mem} = 10^{-7}S/m
ε_{mem} = 3
Live
σ_{cyt}=0.44
ε_{cyt}=60
t_{per}=10nm
σ_{per}=2 S/m
ε_{per}=60
Dead
σ_{dead}=0.09 S/m
ε_{dead} = 60

Fig. 5. (a) Configuration of the ellipsoidal shape of an E.coli bacterium assumed in the numerical simulations with (b) a different cross-section for live and dead bacteria. A conductivity of $\sigma_{sol} = 10^{-3}$ S/m is assumed for the surrounding medium.

We use an AC electric signal with an amplitude of V = 50 mV. The amplitude is high enough to measure an electrical response, yet low enough to minimise Joule heating. The current as a function of frequency is calculated for live and dead bacteria and is compared to the case of no bacteria. The study is conducted in a background medium of conductivity S = 10^{-3} S/m. We note that the largest difference is observed around 10 MHz (Fig. 6) where the change of the electrical properties due to morphological change has the strongest electrical impact.

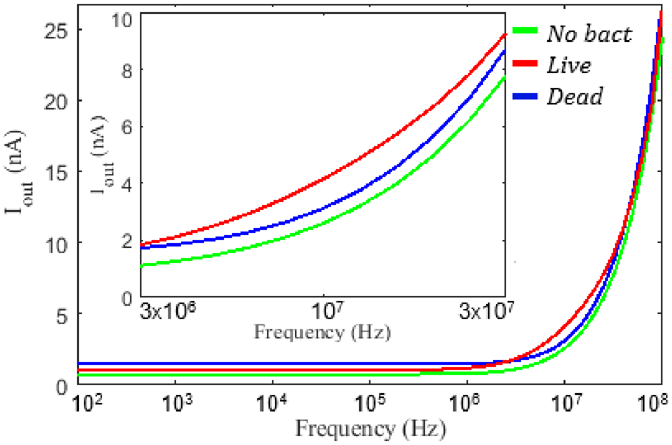

Fig. 6. Current as a function of operating frequency for an empty trap (green curve), a live bacterium (red curve) and a dead one (blue curve).

At low frequency (f < 10 kHz), there is little change in the current obtained for live and dead bacteria because the field is strongly confined at the surface of the silicon slab without directly interacting with the bacterium. A negligible difference of the electrical properties is equally observed for very high frequencies (f > 1 GHz), because the electric field can easily penetrate into the solution without being limited by the bacterium. At f = 10MHz, the current variation is largest with ΔI = 40% between live (I_{live} = 4.2 nA) and dead (I_{dead} = 3 nA) bacteria, corresponding to a detectable difference of 1.2 nA, as verified by the analysis on the current density with a penetration of the electric field in a live bacterium which becomes negligible for a dead one, due to the ions release in the surrounding medium (see Fig. 7).

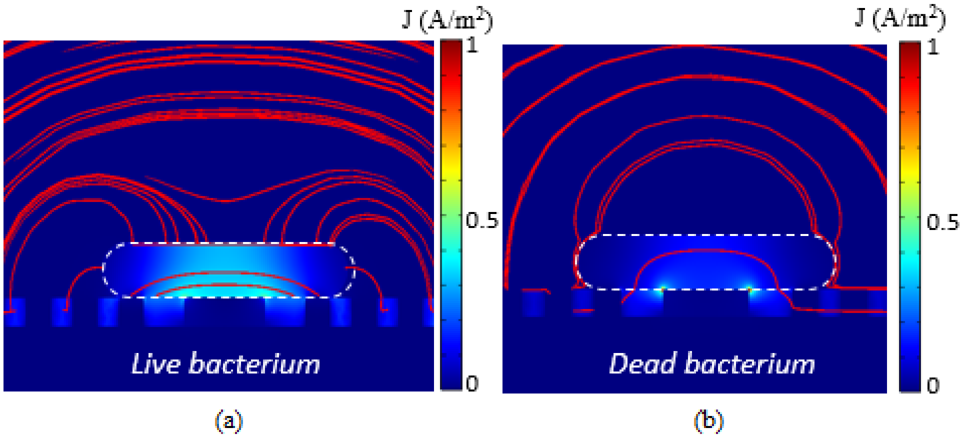

Fig. 7. Current density in the cavity upon trapping (a) a live and (b) a dead bacterium for an AC signal of f = 10 MHz. This frequency produces the largest difference in electrical response, as highlighted by the concentration of streamlines in the bacterium (red lines).

Conclusions

We have introduced the novel concept of a multiparameter, electro-photonic platform that allows monitoring the response of bacteria to antibiotic challenge. The platform is based on an array of nanophotonic traps using photonic crystal cavities. The silicon is partially doped to also enable impedance measurements, which altogether can detect three different responses of bacteria, namely a) changes to their optical density, caused e.g. by changes to the cell wall, b) changes to their motility, which is a very common signature of antimicrobial susceptibility, and c) changes to their metabolic activity, assessed via impedance measurements. This combination of responses allows assessing a wide range of different bacteria and their response to a variety of antibiotics. By arraying the cavities, we can also obtain multiple signatures in parallel and increase the chance of obtaining measurable signals in case of very weak interaction. Since the proposed electro-photonic platform operates on individual bacteria, unlike most other techniques that are based on culturing, it offers a fast time response that could significantly speed up diagnosis, ideally down to timescales of minutes or tens of minutes.

Appendix

Design of the photonic device

The L3-cavity is realized in 220 nm thick SOI and the cavity parameters are specified in Fig. 8. The silicon on either side of the cavity is doped to a concentration of 10^{21} cm^{-3} at the surface ($\sigma = 8.5\text{x}10^5$ S/m) with an exponential drop-off to 10^{17} cm^{-3} within 20 nm ($\sigma = 5.15$ x10^2 S/m), which can be achieved by thermal diffusion doping [33], in order to minimize the optical loss compared to a homogenous doping profile.

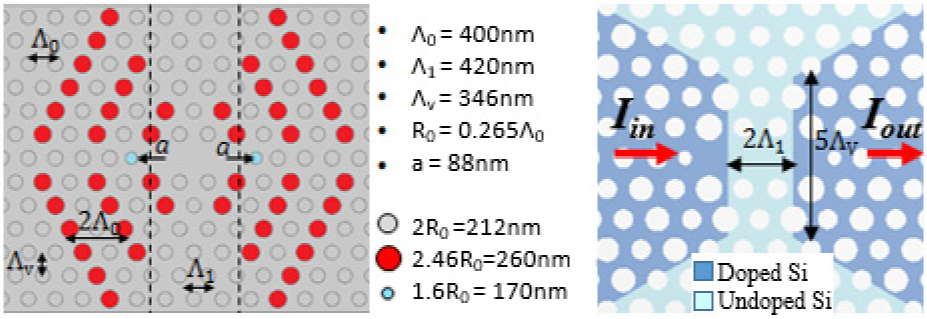

Fig. 8. (a) Geometrical parameters of the PhC L3-cavity configuration and (b) illustration of the doping concentration in the silicon slab ($N_{surface}$ = 10^{21}cm^{-3}) with a region of intrinsic silicon in the centre of the L3-cavity.

Disclosures

The authors declare that there are no conflicts of interest related to this article.

References

1. D. Brown, "Antibiotic resistance breakers: can repurposed drugs fill the antibiotic discovery void?" Nat. Rev. Drug Discov. **14**(12), 821–832 (2015).
2. D. Jasovský, J. Littmann, A. Zorzet, and O. Cars, "Antimicrobial resistance-a threat to the world's sustainable development," Ups. J. Med. Sci. **121**(3), 159–164 (2016).
3. M. M. T. Khan, B. H. Pyle, and A. K. Camper, "Specific and rapid enumeration of viable but nonculturable and viable-culturable gram-negative bacteria by using flow cytometry," Appl. Environ. Microbiol. **76**(15), 5088–5096 (2010).
4. M. Arabski, I. Konieczna, E. Tusińska, S. Wąsik, I. Relich, K. Zając, Z. J. Kamiński, and W. Kaca, "The use of lysozyme modified with fluorescein for the detection of gram-positive bacteria," Microbiol. Res. **170**, 242–247 (2015).
5. R. P. Dickson, B. H. Singer, M. W. Newstead, N. R. Falkowski, J. R. Erb-Downward, T. J. Standiford, and G. B. Huffnagle, "Enrichment of the lung microbiome with gut bacteria in sepsis and the acute respiratory distress syndrome," Nat. Microbiol. **1**(10), 16113 (2016).
6. H. Zhou, D. Yang, N. P. Ivleva, N. E. Mircescu, S. Schubert, R. Niessner, A. Wieser, and C. Haisch, "Label-Free in Situ Discrimination of Live and Dead Bacteria by Surface-Enhanced Raman Scattering," Anal. Chem. **87**(13), 6553–6561 (2015).
7. D. Conteduca, C. Reardon, M. G. Scullion, F. Dell'Olio, M. N. Armenise, T. F. Krauss, and C. Ciminelli, "Ultra-high Q/V hybrid cavity for strong light-matter interaction," APL Photonics **2**(8), 086101 (2017).
8. M. Righini, P. Ghenuche, S. Cherukulappurath, V. Myroshnychenko, F. J. García de Abajo, and R. Quidant, "Nano-optical trapping of Rayleigh particles and Escherichia coli bacteria with resonant optical antennas," Nano Lett. **9**(10), 3387–3391 (2009).

9. M. Tardif, J.-B. Jager, P. R. Marcoux, K. Uchiyamada, E. Picard, E. Hadji, and D. Peyrade, "Single-cell bacterium identification with a SOI optical cavity," Appl. Phys. Lett. **109**(13), 133510 (2016).
10. T. van Leest and J. Caro, "Cavity-enhanced optical trapping of bacteria using a silicon photonic crystal," Lab Chip **13**(22), 4358–4365 (2013).
11. M. Safavieh, H. J. Pandya, M. Venkataraman, P. Thirumalaraju, M. K. Kanakasabapathy, A. Singh, D. Prabhakar, M. K. Chug, and H. Shafiee, "Rapid real-time antimicrobial susceptibility testing with electrical sensing on plastic microchips with printed electrodes," ACS Appl. Mater. Interfaces **9**(14), 12832–12840 (2017).
12. W. P. Larson and R. D. Evans, "Changes in the surface tension of broth produced by the growth of bacteria," *Proc. of the Soc. for Experim. Biol. And Medic.,* volume 21 (1923), pp. 133–134.
13. G. N. Stewart, "The changes produced by the growth of bacteria in the molecular concentration and electrical conductivity of culture media," J. Exp. Med. **4**(2), 235–243 (1899).
14. F. David, M. Hebeisen, G. Schade, E. Franco-Lara, and M. Di Berardino, "Viability and membrane potential analysis of bacillus megaterium cells by impedance flow cytometry," Biotechnol. Bioeng. **109**(2), 483–492 (2012).
15. R. Maalouf, C. Fournier-Wirth, J. Coste, H. Chebib, Y. Saïkali, O. Vittori, A. Errachid, J. P. Cloarec, C. Martelet, and N. Jaffrezic-Renault, "Label-free detection of bacteria by electrochemical impedance spectroscopy: comparison to surface plasmon resonance," Anal. Chem. **79**(13), 4879–4886 (2007).
16. F. Salam, Y. Uludag, and I. E. Tothill, "Real-time and sensitive detection of Salmonella Typhimurium using an automated quartz crystal microbalance (QCM) instrument with nanoparticles amplification," Talanta **115**, 761–767 (2013).
17. A. H. Delcour, "Outer membrane Permeability and Antibiotic Resistance," Biochim. Biophys. Acta **1794**(5), 808–816 (2009).
18. L. Yang, Y. Li, C. L. Griffis, and M. G. Johnson, "Interdigitated microelectrode (IME) impedance sensor for the detection of viable Salmonella typhimurium," Biosens. Bioelectron. **19**(10), 1139–1147 (2004).
19. G. Pitruzzello, S. Thorpe, S. Johnson, A. Evans, H. Gadêlha, and T. F. Krauss, "Multiparameter antibiotic resistance detection based on hydrodynamic trapping of individual E. coli," Lab Chip **19**(8), 1417–1426 (2019).
20. S. L. Portalupi, M. Galli, C. Reardon, T. F. Krauss, L. O'Faolain, L. C. Andreani, and D. Gerace, "Planar photonic crystal cavities with far-field optimization for high coupling efficiency and quality factor," Opt. Express **18**(15), 16064–16073 (2010).
21. R. Terisod, M. Tardif, P. R. Marcoux, E. Picard, J.-B. Jager, E. Hadji, D. Peyrade, and R. Houdrè, "Gram-type differentiation of bacteria with 2D hollow photonic crystal cavities," Appl. Phys. Lett. **113**(11), 111101 (2018).
22. G. N. Stewart, "The changes produced by the growth of bacteria in the molecular concentration and electrical conductivity of culture media," J. Exp. Med. **4**(2), 235–243 (1899).
23. C. Ciminelli, D. Conteduca, F. Dell'Olio, and M. N. Armenise, "Design of an optical trapping device based on an ultra-high Q/V resonant structure," IEEE Photonics J. **6**(6), 0600916 (2014).
24. M. B. Rasmussen, L. B. Oddershede, and H. Siegumfeldt, "Optical Tweezers Cause Physiological Damage to Escherichia coli and Listeria Bacteria," Appl. Environ. Microbiol. **74**(8), 2441–2446 (2008).
25. C. L. Lewis, C. C. Craig, and A. G. Senecal, "Mass and density measurements of Live and Dead Gram-Negative and Gram-Positive Bacterial Populations," Appl. Environ. Microbiol. **80**(12), 3622–3631 (2014).
26. D. Conteduca, F. Dell'Olio, C. Ciminelli, T. F. Krauss, and M. N. Armenise, "Design of a high-performance optical tweezer for nanoparticle trapping," Appl. Phys., A Mater. Sci. Process. **122**(4), 295 (2016).
27. P. Y. Liu, K. Chin, W. Ser, T. C. Ayi, P. H. Yap, T. Bourouina, and Y. Leprince-Wang, "Real-Time Measurement of single bacterium's refractive index using optofluidic immersion refractometry," Procedia Eng. **87**, 356–359 (2014).
28. X. Serey, S. Mandal, and D. Erickson, "Comparison of silicon photonic crystal resonator designs for optical trapping of nanomaterials," Nanotechnology **21**(30), 305202 (2010).
29. A. Rohrbach, "Stiffness of optical traps: quantitative agreement between experiment and electromagnetic theory," Phys. Rev. Lett. **95**(16), 168102 (2005).
30. W. Bai, K. S. Zhao, and K. Asami, "Dielectric properties of E. coli cell as simulated by the three-shell spheroidal model," Biophys. Chem. **122**(2), 136–142 (2006).
31. R. Hölzel, "Non-invasive determination of bacterial single cell properties by electrorotation," Biochim. Biophys. Acta **1450**(1), 53–60 (1999).
32. M. Varshney, Y. Li, B. Srinivasan, and S. Tung, "A label-free, microfluidics and interdigitated array microelectrode-based impedance biosensor in combination with nanoparticles immunoseparation for detection of Escherichia coli O157:H7 in food samples," Sens. Actuators B Chem. **128**(1), 99–107 (2007).
33. P. Cardile, G. Franzo, R. Lo Savio, M. Galli, T. F. Krauss, F. Priolo, and L. O' Faolain, "Electrical conduction and optical properties of doped silicon-on-insulator photonic crystals," Appl. Phys. Lett. **98**(20), 203506 (2011).

193.204.61.220 {ts '2019-07-29 05:54:14'}